ELSEVIER

Polymer 43 (2002) 2191–2200

polymer

www.elsevier.com/locate/polymer

Dynamics of novel hydrogen-bonded acidic fluorinated poly(amide-imide-silica) hybrids studied by solid-state NMR

G.P. Wang[a], T.C. Chang[a,*], Y.S. Hong[a], Y.S. Chiu[b]

[a]*Department of Applied Chemistry, Chung Cheng Institute of Technology, NDU, Tahsi, Taoyuan 335, Taiwan, ROC*
[b]*Chemical Systems Research Division, Chung Shan Institute of Science and Technology, Lungtan, Taoyuan 325, Taiwan, ROC*

Received 23 October 2001; received in revised form 4 December 2001; accepted 21 December 2001

Abstract

Novel hydrogen-bonded acidic fluorinated poly(amide-imide-silica) hybrid materials, FPAI-SiO_2 (6E and 6F) series, were synthesized by a sol–gel process. The structures and spin relaxation of the hybrids were characterized by infrared (IR), and ^{29}Si and ^{13}C nuclear magnetic resonance (NMR) spectroscopy. The abundant Q^4 structures implied that in free catalyst the degree of condensation of tetramethoxysilane was enhanced by hydrogen-bonded acidic fluorinated poly(amide-imide). The dynamics on the local mobility of the hybrids was investigated by the time constant for energy exchange between ^1H and ^{29}Si spin system (T_{SiH}) and spin-diffusion path length (L) measurements. It was found that the faster T_{SiH} of 6E and 6F hybrids compared with the previous study of similar 6C and 6D hybrids implied that 6E and 6F hybrids had more aggregated structures even though the organic terminal segment changed from rigid imide to more flexible amide. The interactions of the charge transfer between donor and acceptor molecules or π–π aromatic stacking may be the dominant factors to affect the structures of 6E and 6F hybrids. Moreover, M^1 and D^2 segments of 6F hybrids had the same level mobility and the mobility of the 6F hybrids was little improved as the soft and flexible 1,3-bis(3-aminopropyl)-tetramethyl-disiloxane segment was incorporated in the dense structures of 6F hybrids. All of the L values of 6E and 6F hybrids were on the scale of 3.5–4.0 nm. The result also suggested that 6E and 6F hybrids had similar denser structures as 6D hybrids.

Keywords: Poly(amide-imide-silica); Hybrid; ^{29}Si-NMR

1. Introduction

Organic polymers combining with inorganic oxides using variations of the sol–gel method have become prevalent for the past 10 years as a means of preparing organic–inorganic hybrid materials [1]. The new hybrid materials would have a controllable combination of the properties of both organic polymers and inorganic glasses [2,3].

Aromatic polyimides are of great interest for high-performance applications, since they exhibit outstanding key properties, such as thermo-oxidative stability, high mechanical strength, high modulus, excellent electrical properties, and superior chemical resistance [4,5]. Particularly, fluorine-containing polyimides have attracted much attention as potential materials for gas separation membranes due to trifluoromethyl (CF_3) groups [6]. However, the major drawbacks of aromatic polyimides for versatile applications are their high melting points and insolubility for organic solvent. To improve the limitation of processing, several attempts have been proposed, such as flexible bridge units or bulky group incorporatation [7,8] and copolymerization modification [9,10]. Unfortunately, their thermal stabilities are depressed. Polyamideimides (PAIs) can increase solubility and retain outstanding mechanical properties and thermo-stability [5,11]. Therefore, PAI is one of the promising approaches [12–14]. PAIs and their hybrids via sol–gel process were prepared and utilized in liquid crystalline polymers [15], second-order non-linear optical polymers [16], and gas separation [17–21].

The solid-state nuclear magnetic resonance (NMR) can provide a powerful method for studying the miscibility, intermolecular interactions, and morphology of polymer blends and copolymerization at near the molecular level by examining NMR parameters [22–29]. Mikawa et al. investigated the gas transport properties and molecular motions of 6FDA (4,4′-(hexafluoroisopropylidene) diphthalic anhydride) copolyimide [30]. They found that the gas transport property increased as the bulky CF_3 group contents of 6FDA copolyimides increased, while the motion of the aromatic carbon was restricted because of the interactions

* Corresponding author. Tel.: +886-3-389-1716; fax: +886-3-389-2711.
E-mail address: techuan@ccit.edu.tw (T.C. Chang).

0032-3861/02/$ - see front matter
PII: S0032-3861(02)00016-2

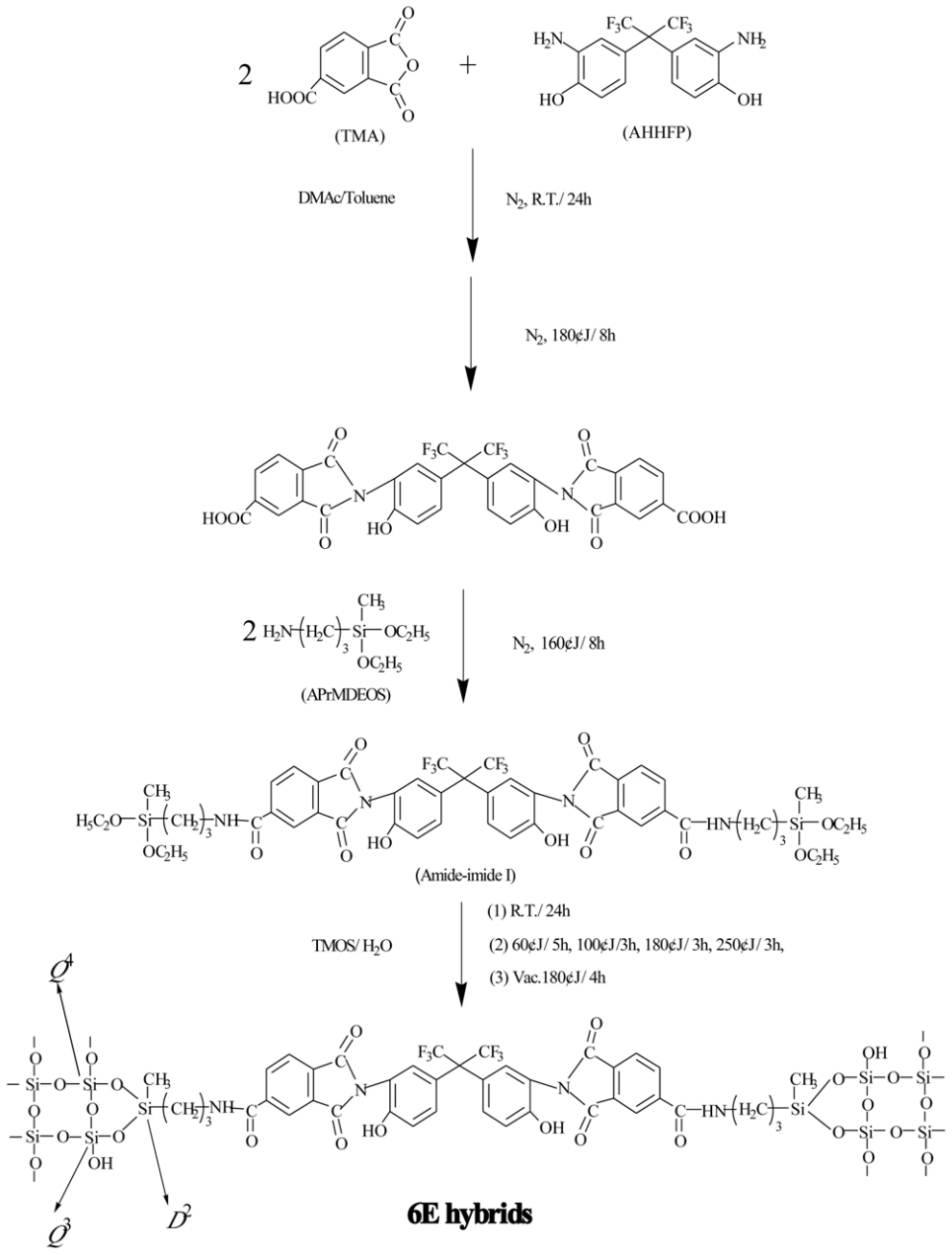

Scheme 1.

such as the charge transfer complex between donor and acceptor molecules or π–π aromatic stacking. In our previous papers [31,32], two types of acidic fluorinated poly(siloxane-imide-silica) hybrids FPAI-SiO_2 (6C and 6D) were prepared from amic acid precursors connected with diethoxysilane via sol–gel method. We found that *L* values (spin diffusion path length) of 6C hybrids were dependent on tetramethoxysilane (TMOS) contents, while those of 6D hybrids were independent of TMOS contents, when the flexible 1,3-bis(3-aminopropyl)-tetramethyl-disiloxane (APrTMDS) segment was incorporated into 6D hybrids. However, the effect of molecular structures to the dynamics of FPAI hybrids was seldom reported by solid-state NMR.

For investigating the effect of molecular structure on the mobility of FPAI hybrids, in the present study we replace 6FDA with trimellitic anhydride (TMA) to reduce bulky group CF_3 contents and change the organic terminal segments from anhydride to acid. Two types of novel hybrids, hydrogen-bonded acidic fluorinated poly(amide-imide-silica) (FPAI-SiO_2 6E and 6F), are prepared by mixing solution of TMOS and diethoxysilane-terminated amideimide (I and II) via sol–gel method. Infrared (IR), ^{13}C-NMR, and ^{29}Si-NMR spectra have characterized the FPAI-SiO_2 hybrid materials. To understand the dynamic behaviors of four types hybrids (6C, 6D, 6E, and 6F), we measured the energy exchange time (T_{SiH}) and the spin-diffusion path length (*L*).

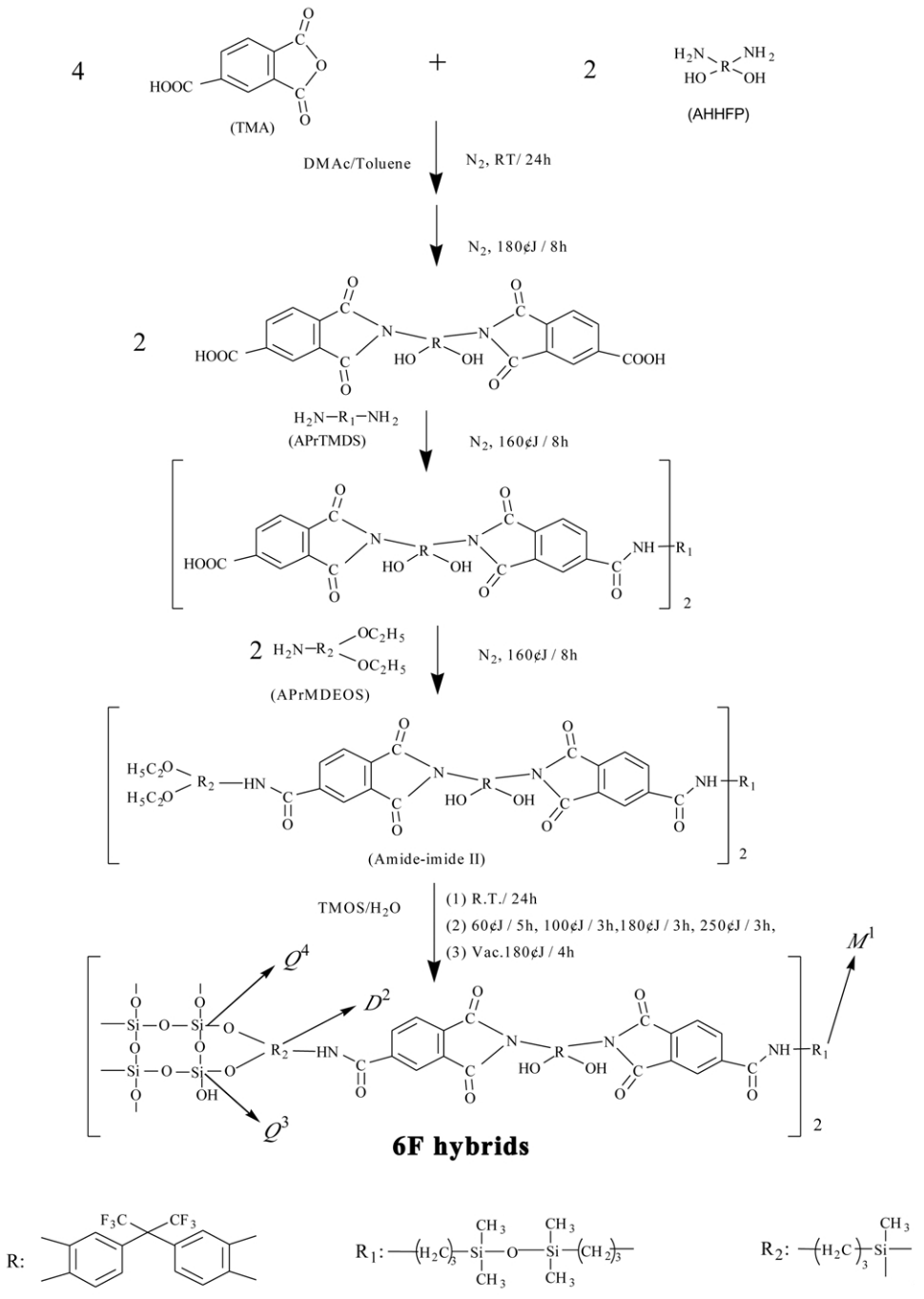

Scheme 2.

2. Experimental

2.1. Materials

2,2′-Bis(3-amino-4-hydroxyphenyl)hexafluoropropane (AHHFP) was obtained in high purity from Chriskev Inc. and dried under a vacuum for 24 h at 70 and 120 °C, respectively. TMOS, 3-aminopropylmethyl-diethoxysilane (APrMDEOS), TMA and APrTMDS were obtained from the Tokyo Chemical Industry Co., and used without further purification. *N*,*N*-Dimethylacetamide (DMAc, Aldrich) and toluene was distilled under a vacuum. Deionized water (18 MΩ) was used for their hydrolysis.

2.2. Preparation of the precursor

The general synthetic scheme of the FPAI-SiO_2 (6E) hybrid materials is depicted in Scheme 1. The preparation of the precursor (diethoxysilane-terminated amideimide (I)) with concentration of 15% solid by weight in solvent was

Table 1
Experimental conditions for poly(amide-imide-silica) hybrid materials (TMA: trimellitic anhydride; AHHFP: 2,2′-bis(3-amino-4-hydroxyphenyl)hexafluoropropane; APrTMDS: 1,3-bis(3-aminopropyl)-tetramethyl-disiloxane; APrMDEOS: 3-aminopropylmethyl-diethoxysilane; and TMOS: tetramethoxysilane)

Hybrids	TMA (mmol)	AHHFP (mmol)	APrTMDS (mmol)	APrMDEOS (mmol)	TMOS (wt%)
6E	8	4	0	8	0
6F	8	4	2	4	0
6E-25	8	4	0	8	25
6F-25	8	4	2	4	25
6E-30	8	4	0	8	30
6F-30	8	4	2	4	30
6E-35	8	4	0	8	35
6F-35	8	4	2	4	35
6E-40	8	4	0	8	40
6F-40	8	4	2	4	40
6E-45	8	4	0	8	45
6F-45	8	4	2	4	45

conducted under nitrogen. The desired amount solution of TMA in a 3:1 (v/v) DMAc/toluene mixture was added to a solution of AHHFP in cosolvent (DMAc/toluene = 3:1) mixture in a round-bottomed flask with a stirring magnet at room temperature about 24 h. The solution was heated with reflux at 180 °C for 8 h, and then APrMDEOS were added and heated at 160 °C for another 8 h. The diethoxysilane-terminated amideimide (I) was thus obtained. The FPAI-SiO_2 (6F) hybrid materials following Scheme 2 were prepared. As described earlier, the same cosolvent and apparatus were used. The desired amount of TMA and AHHFP were dissolved in cosolvent under nitrogen at room temperature about 24 h. The clear solution was heated with fluxed at 180 °C for 8 h, and then APrTMDS were added and heated at 160 °C for 8 h. APrMDEOS was added the last and heated at 160 °C for another 8 h. Finally, the precursor (diethoxysilane-terminated amideimide (II)) was obtained.

2.3. Preparation of the hybrids

The desired amount of water and TMOS were added to the diethoxysilane-terminated amideimide (I) and (II) solution and stirred for an additional 24 h at room temperature. The resulting homogeneous solution was poured onto a Teflon dish. After drying at 60 °C for 5 h and 100 °C for 3 h under atmospheric pressure, the film was ground to powder, and then the power was heated under atmospheric pressure 3 h at 180 °C, 3 h at 250 °C, and 4 h at 180 °C under a vacuum. Hybrid materials were designated so that, for example, 6E-25, 6F-25, 6E-30, 6F-30, 6E-35, 6F-35, 6E-40, 6F-40, 6E-45 and 6F-45, denote diethoxysilane-terminated amideimide (I) and (II) solutions reacted with about 25, 30, 35, 40, 45 wt% of TMOS, respectively, in which the molar ratio of [H_2O]/[TMOS] was 6. The FPAI-SiO_2 6E and 6F hybrids without addition of TMOS were also synthesized via a similar procedure for comparison. The experimental conditions for FPAI-SiO_2 hybrids discussed in this article are shown in Table 1.

2.4. Characterization of the hybrids

The IR spectra of samples dispersed in dry KBr pellets were recorded between 4000 and 550 cm^{-1} on a Bomen DA 3.002 FTIR spectrometer. Imidization and polycondensation were confirmed by the IR spectra of samples. The ^{29}Si and ^{13}C-NMR (Bruker MSL-400) spectra of the solid hybrids were determined by using the cross-polarization combined with magic angle spinning (CP-MAS) technique. The ^{29}Si-NMR provides a unique way to follow the hydrolysis and condensation reactions of silicon alkoxides. The nomenclatures of M^i, D^i, and Q^i are taken from Glaser and Wilkes [33], where i refers to the number of –O–Si groups bounded to the silicon atom of interest. M^i, D^i, and Q^i denote species that have three, two and no organic side group, respectively.

CP contact time studies can produce the Si–H polarization transfer time constant (T_{SiH}). The ^1H–^{29}Si spin contact time with the Hartmann–Hahn condition fulfilled in the rotating frame was typically about 5 ms, but was optimized in a range of 0.5–20 ms. The spin–lattice relaxation times in the rotating frame ($T_{1\rho}^H$) were measured with a ^1H spin-lock τ-pulse sequence followed by CP. The ^1H 90° pulse widths were 4.5 μs, and the CP contact time was 2 ms. The length of delay time τ ranged from 0.1 to 25 ms for $T_{1\rho}^H$.

3. Result and discussion

3.1. Structural characterization

The hybrids present the silanol group formed during the hydrolysis of alkoxy groups (Si–OCH_3) in APrMDEOS and TMOS, and that induces cross-linked three-dimensional (3D, Q^i) network materials. However, the 6E and 6F hybrids present two siloxane bonds and one methyl group bonded to silicon atom, giving a 2D network material. The theoretical schematic structures of the hybrids are shown in Schemes 1 and 2. IR and

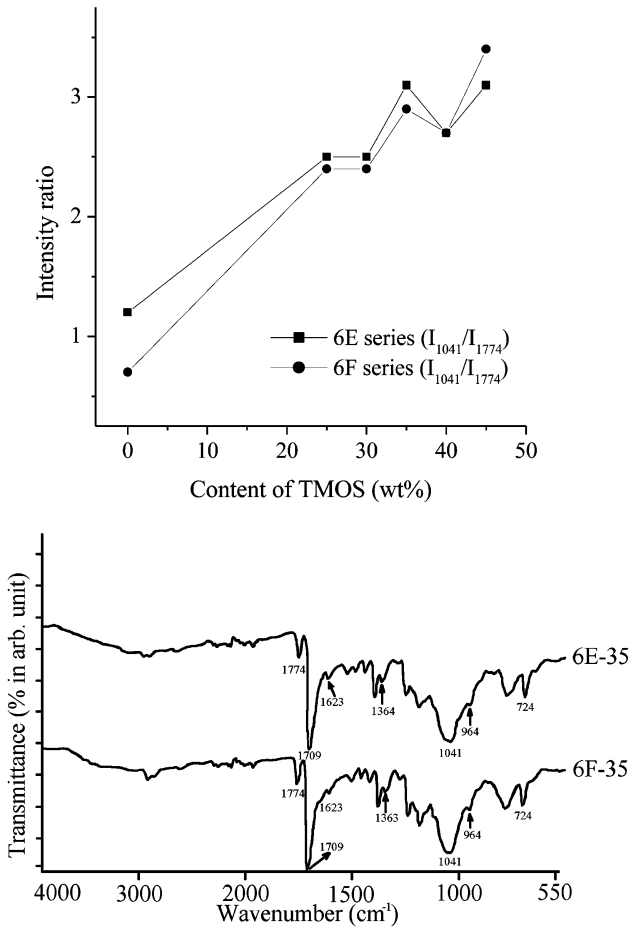

Fig. 1. IR spectra of the FPAI-SiO_2 hybrid materials 6E-35, 6F-35, as well as the ratio of intensity I (1041 cm^{-1}) of Si–O–Si to the reference imide band (1774 cm^{-1}) of the hybrids.

solid-state ^{29}Si-NMR provide evidence for the formation of hybrid network materials.

All hybrids present the characteristic imide peaks (Fig. 1) at 1774 (imide C=O symmetric stretching), 1709 (imide C=O asymmetric stretching), 1364 (C–N imide stretching), and 724 cm^{-1} (imide ring deformation), and a weak amide C=O stretching (1623 cm^{-1}). The absorptions in the range 3700–3200 and 964 cm^{-1} are the characteristic band of silanol groups (Si–OH) that are formed during the hydrolysis of alkoxy groups in APrMDEOS or TMOS. The carbonyl stretching bands in FPAI-SiO_2 hybrids are shifted to lower wave number (1774 and 1709 cm^{-1}) as observed from a comparison with in 5-member imide ring (1782 and 1724 cm^{-1}). The result suggests that a hydrogen bond is formed between the amideimide moieties and the silanol group in FPAI-SiO_2 hybrids [34]. On the other hand, the absorption of Si–O–Si vibration (1041 cm^{-1}) is weak in 6E and 6F polymers, but this absorption band becomes stronger with increasing TMOS contents for 6E and 6F hybrids. The result implies the condensation of the already hydrolyzed TMOS forms the 3D Si–O–Si network [35]. The intensity ratio of the Si–O–Si (Fig. 1) to the reference imide vibration (1774 cm^{-1}) increases roughly with the increasing of TMOS contents. Moreover, at the same TMOS content the intensity ratio of 6E hybrids is almost higher than that of 6F. This result suggests that at the same condition the condensation of 6E hybrids is more than that of 6F hybrids.

Fig. 2(A) shows the ^{13}C CP-MAS NMR spectrum of 6E polymer. A set of peaks is observed at 167, 151, 141–110 and 64 ppm that are arise from the imide carbonyl, aryl carbons with hydroxyl groups, various aromatic carbons and trifluoromethyl carbons, respectively [36]. Moreover, the other set of peaks are observed at around 40, 22, 14, and −1.3 ppm that correspond to $-NCH_2-$, $-CH_2-$, $-CH_2Si-$, and $-SiCH_3$, respectively. Fig. 2(B) shows the ^{13}C CP-MAS NMR spectrum of 6F polymer. The ^{13}C CP-MAS NMR spectra of FPAI-SiO_2 6E and 6F polymers are nearly identical, and they have sufficient resolution to identify peaks. The corresponding carbon structures of the peaks are all assigned in Fig. 2(A) and (B).

The ^{29}Si-NMR spectrum of 6E-30 hybrid (Fig. 3) shows two peaks about at −17 and −106 ppm corresponding to D^2 and Q^4, respectively. Moreover, a shoulder shows at about −100 ppm that corresponds to Q^3 structure [37]. The D^2 structures and Q^i structures ($i = 3$ and 4) can be attributed to the silicon in the siloxane sequence and 3D silica network, as shown in Scheme 1. The degree of condensation (D_c) of the TMOS, determined by a quantitative analysis of the D^2, Q^3, and Q^4 resonance signals, can be calculated. The actual degree of condensation (D_c) evaluated from the proportions of D^i and Q^i species according to the following equation:

$$D_c(\%) = \left[\frac{D^1 + 2D^2}{2} + \frac{Q^1 + 2Q^2 + 3Q^3 + 4Q^4}{4} \right] 100 \quad (1)$$

It is found that the D_c values of all hybrids of 6E and 6F are more than 95% and TMOS condensation is almost complete in the absence of HCl in hybrids. The results imply that the fluorinated PAI is acidic. On the other hand, the ^{29}Si-NMR spectrum of 6F-30 hybrid (Fig. 3) shows three peaks about at 13, −17 and −109 ppm corresponding to M^1, D^2, and Q^4, respectively. A shoulder also shows at about −101 ppm that corresponds to Q^3 structure. The M^1, D^2 and Q^i structures ($i = 3$ and 4) can be also attributed to the silicon in the siloxane segments and the silica network as shown in Scheme 2.

3.2. ^{29}Si cross-polarization dynamics

In the conventional CP process under Hartmann–Hahn conditions, ^{1}H and ^{29}Si spin systems are spin-locked in the rotating frames and thermally in contact with each other, thus exchanging their energies. The respective spin systems also exchange energies with the surrounding thermal reservoir, the so-called lattice. Fig. 4 gives an example of the effect of contact time (t) on the ^{29}Si resonance of 6E-30 and 6F-30 hybrids. Intensities (Fig. 4) reflect local cross-polarization

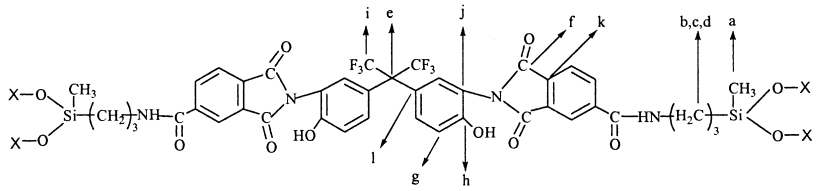

6E copolymer X: CH_3 or H

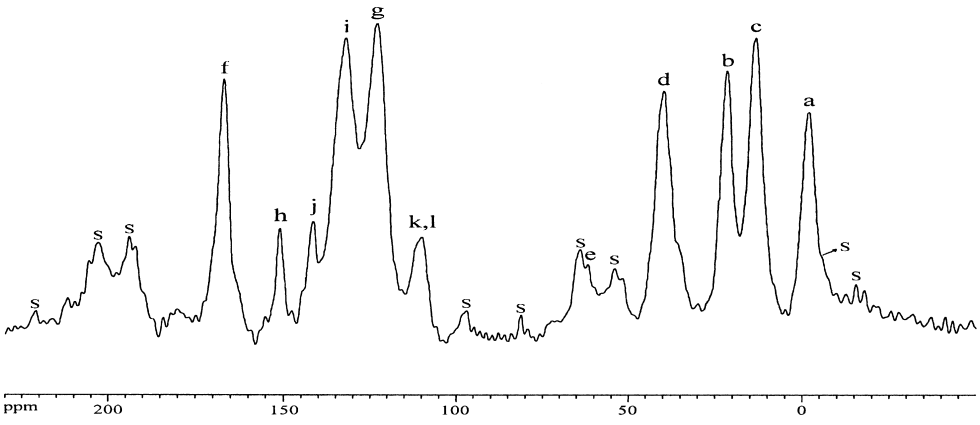

(2A)

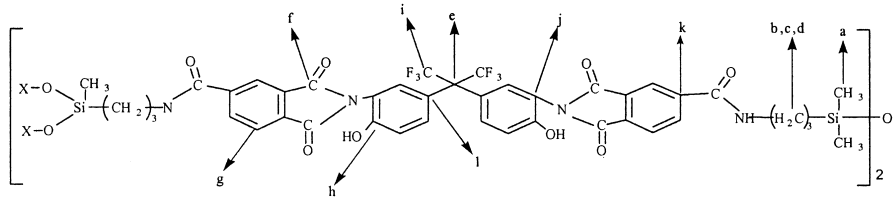

6F polymer X : CH_3 or H

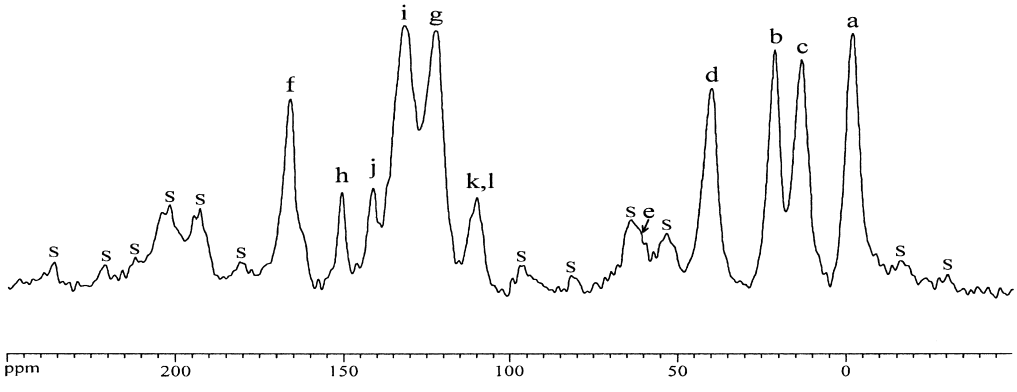

(2B)

Fig. 2. CP-MAS ^{13}C-NMR spectrum of the 6E (A) and 6F (B) copolymer (s: side band).

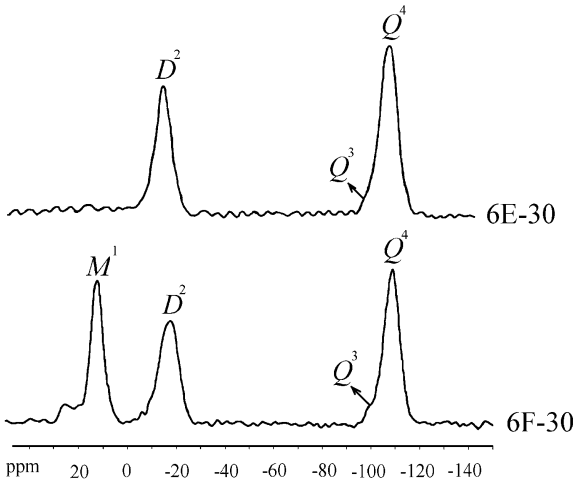

Fig. 3. CP-MAS ^{29}Si-NMR spectrum and structure of the 6E-30 and 6F-30 hybrids.

dynamics that may vary from site to site. According to the simple theory in this CP process, magnetization, M_c (t), is expressed as a function of the contact time as follows [38]:

$$M_c(t) = M_e\left[\exp\left(-t/T_{1\rho}^H\right) - \exp(-t/T_{SiH})\right] \quad (2)$$

Here, M_e is the ^{29}Si equilibrium magnetization obtained, when both spin systems fully interact with each other without any energy exchange with the lattice. T_{SiH} is the time constant for the energy exchange between ^{1}H and ^{29}Si spin systems, and $T_{1\rho}^H$ is the spin–lattice relaxation time in rotating frame. This equation indicates that the ^{29}Si magnetization appears at the rate of the order of $(T_{SiH})^{-1}$ and disappears at the rate of $(T_{1\rho}^H)^{-1}$. The rate of polarization transfer is dependent upon the distance between silicon and hydrogen atoms and on local motion. Silicon atoms, which are far from protons or very mobile, will take a longer time to cross-polarize.

Fig. 5 gives an example to show the semi-logarithmic plot of the peak intensity as a function of the contact time for the silicon in the 6E-30 and 6F-30 hybrids, respectively. In Fig. 5, a steeper slope is an indication of faster transfer of magnetization (shorter T_{SiH}) or faster relaxation by spin diffusion (shorter $T_{1\rho}^H$). The D^2 and M^1 structures with the largest number of relatively close protons should exhibit the shortest T_{SiH} values, while Q^4 structures lack of directly bonded protons should have the longest T_{SiH} as compared to the D^2 and M^1 structures. However, the conversely results suggest that the greater motion of the D^2 and M^1 segments could result in weak dipolar coupling and longer T_{SiH} relaxations. Moreover, the linear curves of Q^4 species is shown in Fig. 5, the result suggests that macroscopic phase separation does not occur in these materials.

3.3. Comparison of four kinds hybrids dynamic behavior

Four series of hybrids (6C, 6D, 6E, and 6F) are prepared in our laboratory. Their structures are shown in Scheme 3.

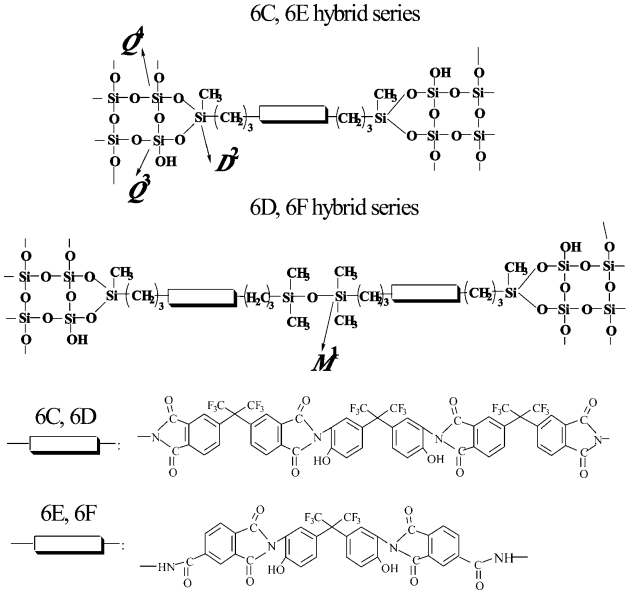

Scheme 3.

Basically, there are two kinds of organic segments shown as blocks for the hybrids. 6C and 6D Hybrids are made from 6FDA, and 6E and 6F are composed by TMA. The difference between (6C, 6E) and (6D, 6F) is that the latter have the flexible soft aliphatic *n*-propyl Si–O–Si (APrTMDS) segments. The T_{SiH} values of all hybrids are plotted in Figs. 6 and 7. By comparing with the hybrids' T_{SiH} values estimated by curve fitting, the dynamic behaviors of the four kinds hybrids can be studied.

There are two competitive factors to affect the molecular interactions in these hybrids. One is CF_3 bulky group or flexible amide and APrTMDS segment to increase molecular mobility and free volume; the other is the charge transfer complex or π–π aromatic stacking of imide segments to aggregate molecular structure [30]. From the molecular structures of Scheme 3, we predict that 6F series should have the most flexible structure and the longest T_{SiH}. However, 6E and 6F had the shorter T_{SiH}, as observed from a comparison with 6C and 6D. The converse results imply that both 6E and 6F should have more aggregated structures even though the rigid imide segments of 6E and 6F hybrids changed to more flexible amide segments. It is also interesting to note that M^1 and D^2 of 6F hybrids have the same level T_{SiH} (Fig. 7), the result suggests that M^1 (soft and flexible APrTMDS segment) and D^2 (organic and inorganic interface segment) of 6F hybrids have the same level mobility and the incorporation of flexible APrTMDS to 6F hybrids has little mobility improvement. The results may be rationalized on the inference that in 6E and 6F hybrids the interactions, such as the charge transfer complex between donor and acceptor molecules or π–π aromatic stacking, may be the dominant factors to make PAI hybrid structures more aggregated, when bulky group CF_3 content decreased. Furthermore, the spin-diffusion path length (L) can be

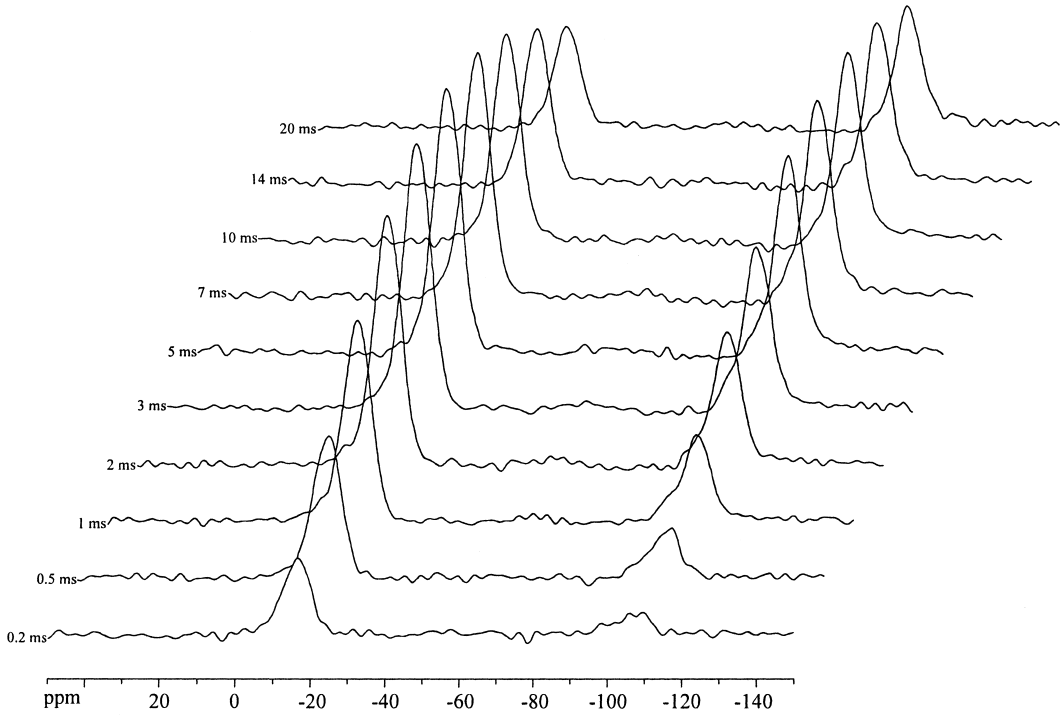

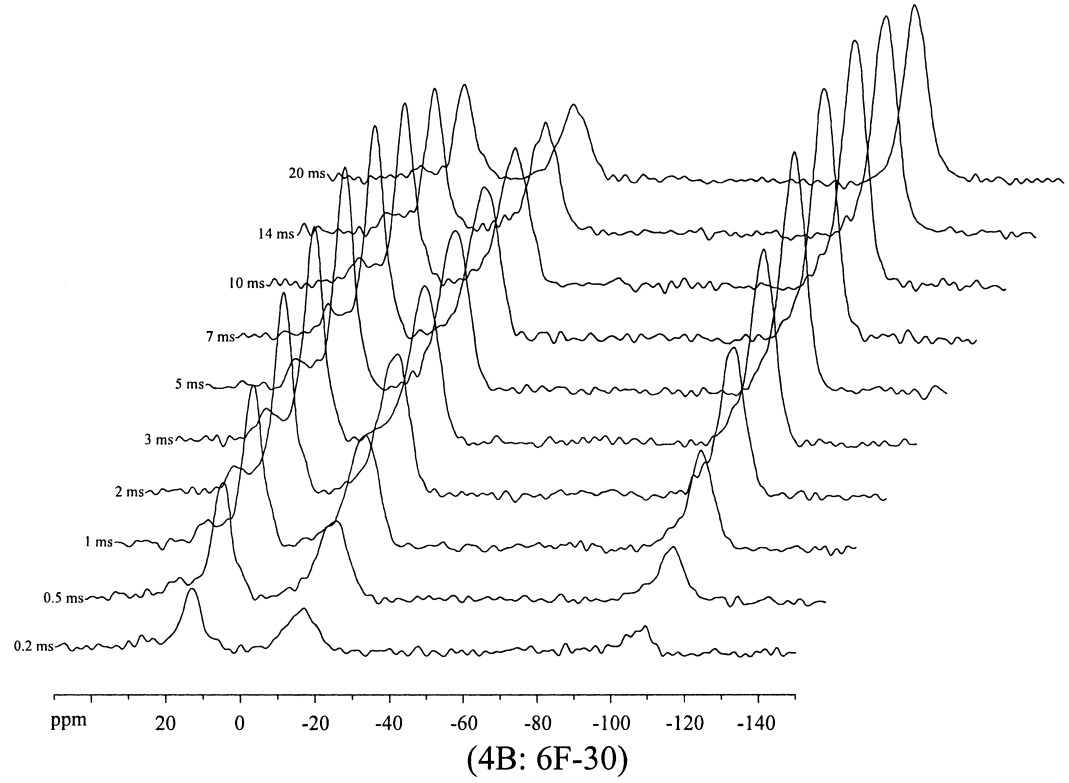

Fig. 4. Stacked plot of the CP-MAS ^{29}Si-NMR spectra of 6E-30 (A) and 6F-30 (B) hybrids as a function of contact time.

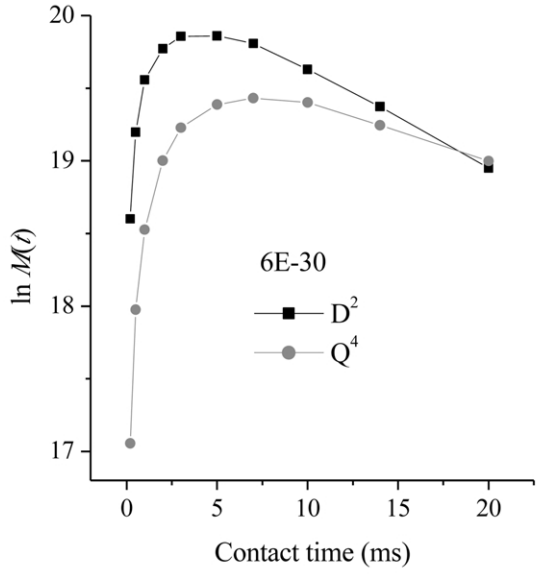

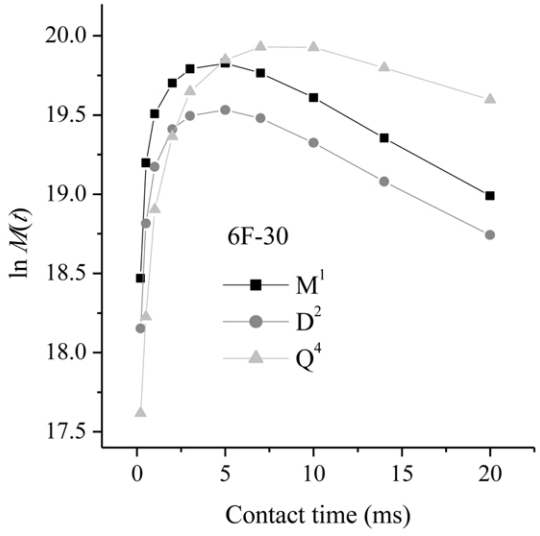

Fig. 5. 6E-30 and 6F-30 hybrids peak intensity semi-logarithmic plot of the D^2, M^1, and Q^4 species shown in Fig. 4 as a function of the contact time.

estimated using the following equation [38]:

$$L = \left(6DT_{1\rho}^{\mathrm{H}}\right)^{1/2} \tag{3}$$

Here D is the effect spin-diffusion coefficient depending on the average proton to proton distance, as well as dipolar interaction and it has a typical value of the order of $10^{-16}\,\mathrm{m^2\,s^{-1}}$. The L value is one of the good methods to estimate the upper limit of the domain size in the homogeneous study. The L values versus TMOS contents of all hybrids are plotted in Fig. 8. The L values of 6C hybrids decrease as TMOS contents increase, and become near constant, when TMOS contents more than 30 wt%. On the other hand, the L values of 6D hybrids are in the range of 3.0–4.0 nm. However, all of the L values of 6E and 6F

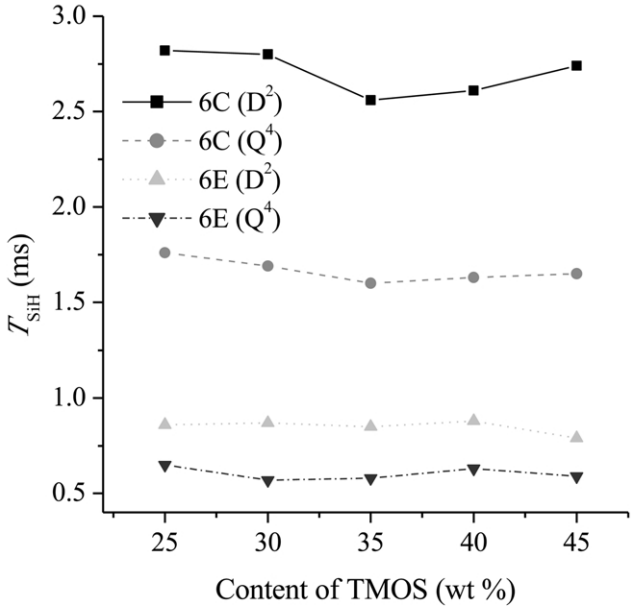

Fig. 6. Plot of T_{SiH} versus TMOS contents of the FPAI-SiO_2 6C and 6E (D^2 and Q^4) hybrid materials.

hybrids are on the scale of 3.5–4.0 nm. The results suggest that 6E and 6F hybrids have similar denser structures as 6D hybrids. We perhaps can infer that 6E and 6F hybrids have the less CF_3 bulky groups and more aggregated structures even though organic terminal segments change from imide to amide. Therefore, the effect of the mobility for soft flexible APrTMDS segment is little exhibited between 6E and 6F series hybrids. On the other hand, 6C and 6D hybrids have more CF_3 bulky group, weaker charge transfer or π–π aromatic stacking interactions, and less aggregated structures. However, the soft flexible APrTMDS segment

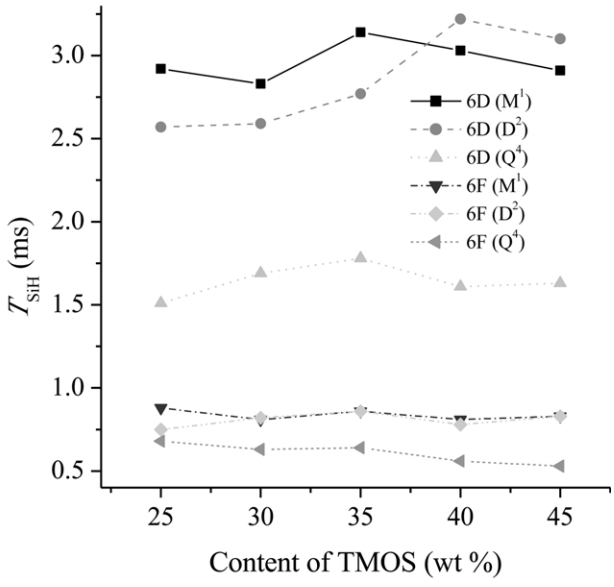

Fig. 7. Plot of T_{SiH} versus TMOS contents of the 6D and 6F (D^2, M^1, and Q^4) hybrid materials.

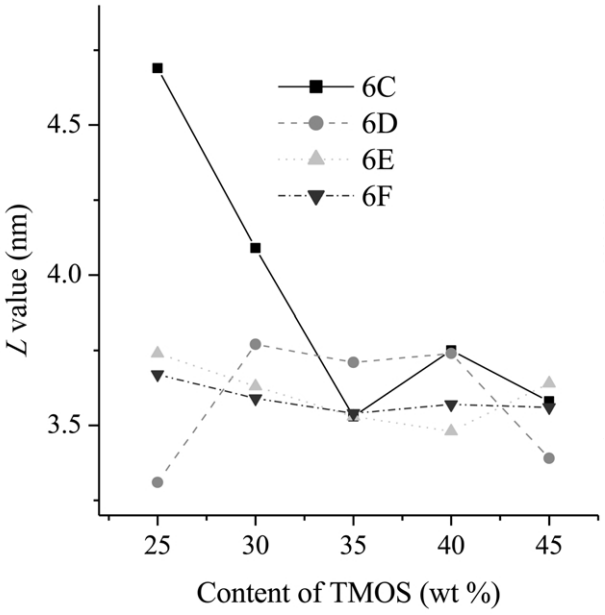

Fig. 8. Plot of L values versus TMOS contents of 6C, 6D, 6E, and 6F hybrid materials.

incorporated into 6D hybrids can exhibit its mobility to rearrange chain segments, enhance the interaction of charge transfer or π–π aromatic stacking, and make the structures of 6D hybrids denser.

4. Conclusions

The novel hydrogen-bonded acidic poly(amide-imide-silica) hybrids (6E and 6F) were prepared and characterized by IR, ^{13}C and ^{29}Si-NMR. The hydrogen-bonded and acidic properties were confirmed by carbonyl group IR absorption band shifted to lower wave number and ^{29}Si-NMR abundant Q^4 structures, respectively. From T_{SiH} and L values, we could infer that 6E and 6F hybrids had aggregated structures, and the interactions of the charge transfer between donor and acceptor molecules or π–π aromatic stacking thus may be the dominant factors to affect the structures of 6E and 6F hybrids. In the dense structures of 6F hybrids, the mobility of M^1 and D^2 was the same level and little improved by the incorporation of soft flexible APrTMDS and the change from rigid imide segments to more flexible amide segments. However, the APrTMDS segment incorporated into 6D hybrids could exhibit its flexibility to rearrange chain segments, enhance the interaction of charge transfer or π–π aromatic stacking, and make the denser structures as compared with 6C hybrids.

Acknowledgements

The authors thank the National Science Council of the Republic of China (Grant NSC 90-CS-7-014-001). We would also like to thank Ms S.Y. Fang (Tsing Hua University) for help in the NMR measurements.

References

[1] Mark JE, Lee CYC, Bianconic PA, editors. Hybrid organic–inorganic composites. ACS Symposium Series 585. Washington, DC: American Chemical Society, 1995.
[2] Loy DA, Shea KJ. Chem Rev 1995;95:1431.
[3] Wen JG, Wilkes L. Chem Mater 1996;8:1667.
[4] Fegar C, Khojasteh MM, Htoo MS, editors. Advances in polyimide science and technology. New York: Technomic Publishing, 1991.
[5] Ghosh MK, Mittal KL, editors. Polyimides: fundamentals and applications. New York: Marcel-Dekker, 1996.
[6] Aoki T. Prog Polym Sci 1999;24:951.
[7] Li YF, Ji T, Zhang J. J Polym Sci, Part A: Polym Chem 2000;38:189.
[8] Liaw DJ, Liaw BY. Polymer 1999;40:3183.
[9] Kricheldorf HR, Wollheim T, Koning CE, Werumeus-Buning HG, Altstädt V. Polymer 2001;42:6699.
[10] Nakamura K, Ando S, Takeichi T. Polymer 2001;42:4045.
[11] Yang CP, Chen RS, Hung KS. Polymer 2001;42:4569.
[12] Yang CP, Chen RS, Chen JA. J Polym Sci, Part A: Polym Chem 2000;38:1.
[13] Lee YB, Park HB, Shim JK, Lee YM. J Appl Polym Sci 1999;74:965.
[14] Hsiao SH, Chang LM. J Polym Sci, Part A: Polym Chem 2000;38:1599.
[15] Tamai S, Ohkawa Y, Yamaguchi A. Polymer 1997;38:4079.
[16] Kim HK, Moon IK, Lee HJ, Han SG, Won YH. Polymer 1998;39:1719.
[17] Xu ZK, Böhning M, Springer J, Steinhauser N, Mülhaupt R. Polymer 1997;38:581.
[18] Ha SY, Park HH, Lee YM. Macromolecules 1999;32:2394.
[19] Lee YB, Park HB, Shim JK, Lee YM. J Appl Polym Sci 1999;74:965.
[20] Hu Q, Marand E, Dhingra S, Fritsch D, Wen J, Wilkes G. J Membr Sci 1997;135:65.
[21] Hu Q, Marand E. Polymer 1999;40:4833.
[22] Kim JH, Kim EJ, Choi HC, Kim CW, Cho JH, Lee YW, You BG, Yi SY, Lee HJ, Han K, Jang WH, Rhee TH, Lee JW, Pearton SJ. Thin Solid Film 1999;341:192.
[23] Chan CK, Chu IM. Polymer 2001;42:6823.
[24] Wang J, Cheung MK, Mi Y. Polymer 2001;42:2077.
[25] Lin RH, Woo EM, Chiang JC. Polymer 2001;42:4289.
[26] Nakaoki T, Ohira Y, Horii F. Polymer 2001;42:4555.
[27] Brus J, Dybal J. Polymer 2000;41:5269.
[28] Hou SS, Kuo PL. Polymer 2001;42:9505.
[29] Yi JZ, Goh SH. Polymer 2001;42:9313.
[30] Mikawa M, Nagaoka S, Kawakami H. J Membr Sci 1999;163:167.
[31] Chang TC, Wang GP, Tsai HC, Hong YS, Chiu YS. Polym Degrad Stab 2002;74:229.
[32] Chang TC, Wang GP, Tsai HC, Hong YS, Chiu YS. J Polym Anal Character 2002 in press.
[33] Glaser RH, Wilkes GL. Polym Bull 1988;19:51.
[34] Ahn T, Kim M, Choe S. Macromolecules 1997;30:3369.
[35] Avadhani CV, Chujo Y, Kuraoka K, Yazawa T. Polym Bull 1997;38:501.
[36] Smaihi M, Schrotter JC, Lesimple C, Prevost I, Guizard C. J Membr Sci 1999;161:157.
[37] Wu KH, Chang TC, Wang YT, Chiu YS. J Polym Sci Polym Chem 1999;37:2275.
[38] Mehring M. Principles of high resolution NMR in solids. 2nd ed. Berlin: Springer, 1983.